PDR

Acute Lesions In Skin Produced By Radioactive Microspheres

I. ^{235}Uranium-Carbide Microspheres

P. Donald Forbes [1] and S. Z. Mikhail [2,3]

1. The Skin and Cancer Hospital
Temple University Health Sciences Center
3322 North Broad Street
Philadelphia, Pennsylvania 19140

2. U.S. Naval Radiological Defense Laboratory
San Francisco, California 94135

3. Present Address:
Naval Electronics Laboratory
271 Catalina Boulevard
San Diego, California 92152

Parts of this work supported by Contracts
ERDA E(11-1)-2366, SNPN-49,
USNRDL N00 228 68 C 0571 and N00 69 C 1303
And by NIH Grants ES 00269 and CA 11536

TABLE OF CONTENTS

LIST OF FIGURES

LIST OF TABLES

ABSTRACT

Tissue effects were evaluated after activated uranium microspheres were applied to the skin of mice and swine. Radiation doses absorbed in tissue were estimated utilizing a beta extrapolation chamber and the beta "Transmission, Degradation and Dissipation" (TDD) model developed at the Naval Radiological Defense Laboratory. At a point on the circumference of a 4 mm radius circle, 100u below the tissue surface, the doses ranged from 4×10^2 to 3.5×10^4 rads as a function of particle size and exposure time. Ulcers in pig skin began at the site of contact and eventually became 0.5 - 8 mm in diameter. The post-irradiation syndrome also included pigmentation changes, inhibition of hair growth, desquamation, and contraction.

Similar changes were seen in particle-exposed mouse skin, but at significantly lower estimated doses. The inhibition of hair growth was used to calculate a dose-response curve for mouse skin. The results indicate that this system can provide useful biological dosimetry.

Introduction

Assessing the environmental impact of nuclear reactor use involves a variety of problems. One subset of problems relates to uncertainties about effects of radioactive microspheres ("hot particles"). There are few experimental data available on the carcinogenic risk for specific tissues exposed to non-uniform fields of radiation. Charles (1) has recently reviewed the theoretical models which attempt to describe dose distribution and to assign carcinogenic risk in small areas which are heavily irradiated.

Even for acute effects, there are few experimental data available on the changes that might be expected in skin following exposure to a radioactive microsphere. The skin is by no means the sole tissue at risk, nor possibly even the most important. Skin does, however, provide a readily accessible source of both clinical and experimental information.

This study was designed to provide information on the biologic response to hot particle exposure. We investigated damage and repair in the skin of mice and miniature swine, using reactor-activated uranium microspheres. Biologic effects were related to computed radiation distribution in the tissue. A subsequent report (2) will deal with effects from exposure to ^{90}Sr-silicate microspheres.

Materials and Experimental Procedure

Particulate Sources

Materials

Each of the particles used in this study was a pyrolytic graphite-coated microsphere of 93% enriched 235-uranium carbide (UC_2). The particles fell into two distinct size categories. The smaller particles ranged in diameter from 138 to 154 microns (μ). The larger particles had a range in diameter of 277μ to 328μ. These diameters include the graphite coating. Particles of the same size classes were used to determine the thickness of the graphite coating. By applying pressure on a particle placed between two glass slides, the coating was split and removed. Using the sizing technique described below and after removal of the coating, the coating thickness was determined to be between 23μ and 27μ. Thus, for the whole set of UC_2 microspheres used, the approximate *core* diameter ranged from 113μ to 303μ. The diameter shown in Tables II and III includes the graphite coating.

Particle Size Determination

Two photomicrographs (X400) were taken for each particle. Several measurements were made on each, and the average was determined. The particles

appeared to be almost perfectly spherical. In some instances removal of the graphite layer for determination of the coating thickness revealed a little roughness on the UC_2 surface.

Reactor Irradiation

Activation was accomplished in the pneumatic tube facility of pool-type research reactors. The work was undertaken initially at the Rhode Island Nuclear Science Center, Narragansett, Rhode Island, subsequent experiments were run at the Industrial Reactor Laboratory, Plainsboro, New Jersey. The nominal flux of the 5 megawatt IRL reactor was 10^{13} neutrons $cm^{-2}sec^{-1}$.

Animal Experiments

Experimental Design

Experiment A provided the opportunity to test reactor configurations, particle handling techniques, biologic endpoints and measuring devices to be used during subsequent investigations. This experiment involved 20 UC_2 fuel beads, 4 pigs, 38 haired mice, 14 rhino mice, several days' use of reactor facilities, and a variety of equipment and supplies. Dosimetry estimates from the activated particles indicated that the reactor neutron flux was adequate for activation and that the beta flux from the particles was sufficient for biologic work. Subsequent experiments were designed to yield the more precise physical and biological measurements required for dose-response evaluations. For *Experiment B*, 19 particles were activated and placed on two pigs (Fig. 4). The 20 particles used in *Experiment C* were used to irradiate skin on 38 haired mice (Fig. 4, 6, 7) and 10 rhino mice (Fig. 9).

Animal Exposures

Following reactor activation the individual particles were sandwiched between thin films of polyethylene (density: 1.2 mg cm^{-2}), and these packets were taped to the shaved skin of the experimental animals for various periods of time ranging from 5 minutes to 3 hours. In each case, the particle was separated from the skin by the 10-micron thick film. The particles were spaced at distances adequate to insure separate treatment areas.

Miniature swine of the Hanford-Labco Cross variety (Battelle-Northwest Laboratory) are characteristically sparsely haired (3) and they have a variable amount of dark-colored skin. The pigs were approximately 20 kg in weight at the time of exposure. The area selected for study extended from the hip to the shoulder and from the mid-dorsum to a point 30 cm. down each side. Haired mice ($C_{57}BL/10J$) were treated by applying the hot particle to plucked skin during the resting (telogen) phase of the skin cycle.

Rhino mice have no surface hair (4). The treated sites on both mice and swine were permanently identified with tattoo marks; nevertheless, the unique syndrome of changes that accompanied even the smallest ulcers provided positive identification of radiation-induced lesions.

Daily observations were made on the animals during the first month after exposure, and then the detailed examinations were continued twice weekly; photographs were taken during the examinations. Tissue biopsies from some of the exposed areas were examined histologically using a variety of staining techniques (5).

Determination of the Number of Equivalent Fissions

Calculation of the number of fissions occuring in each particle during activation through knowledge of the neutron flux, the fission cross-section, the amount of fissionable material in the particle, and the exact length of activation period was tried but found unsatisfactory. An undue amount of care was required in experimental determination of the integrated thermal, epithermal, and fast neutron flux and in calculating the correction factors due to the shadowing effect particles had on each other. This technique was, therefore, abandoned in favor of direct estimation of the number of fissions in each individual particle by measurement of its total decay gamma radiation in a high pressure ionization chamber. The chamber used is identical to an instrument designed and built at Oak Ridge National Laboratory and described by Jones and Overman (6). A partial description of the ion chamber was given by Miller (7) along with computed energy calibration curves based on the response of the instrument to a number of radionuclides of known disintegration rate and energy level decay scheme. Using the computed calibration curves and the decay schemes of individual fission products, Miller predicted the response of the instrument to decay gamma from fission product mixtures.

Using Miller's computations, Mackin et al. (8) constructed a response curve of current per fission versus time after fission, which they verified experimentally. Their experience with the chamber showed that measurements on representative samples generally agreed within ± 10% of radiochemically determined values of number of fissions.

Instrumental precision was further tested in the following manner. The number of fissions in each of six particles was determined with this chamber and checked by quantitative chemical analysis and gamma counting at Los Alamos Scientific Laboratory. Table I presents the data obtained. As can be seen from Column 7 of the table, the percentage difference between the corresponding values of the number of fissions did not exceed 7%.

Table I

COMPARISON OF FISSION DATA

Particle Number	Particle Diameter	Number of Equivalent Fissions			Difference	Difference % of Average
		NRDL	LASL	Average		
1	285	5.9×10^{12}	5.73×10^{12}	5.84×10^{12}	0.23×10^{12}	3.95
2	312	7.69×10^{12}	7.45×10^{12}	7.57×10^{12}	0.24×10^{12}	3.17
3	295	6.59×10^{12}	6.38×10^{12}	6.48×10^{12}	0.21×10^{12}	3.24
4	152	6.53×10^{11}	6.19×10^{11}	6.36×10^{11}	0.34×10^{11}	5.35
5	149	6.15×10^{11}	5.74×10^{11}	5.94×10^{11}	0.41×10^{11}	6.91
6	147	5.60×10^{11}	5.33×10^{11}	5.44×10^{11}	0.23×10^{11}	4.23

Particles used for animal exposure were transported immediately to NRDL for determination of the number of fissions and beta dose rate. Each particle was placed in a clean thin-walled plastic tube and measured in a 4-pi chamber at least twice within a period of 2 to 5 days following its arrival. Its beta dose rate was determined by the method described in the following section.

Beta Dose-Rate Measurements and Calculations

The Extrapolation Chamber

Dose-rate measurements for each particle were made using an extrapolation chamber of the type described by Loevinger (10). The measurements made were of the ionization within a volume of air of uniform thickness between two tissue equivalent electrodes. The electrode area (5.07 cm^2), and the distance between the electrodes defined the ionization volume(11), Fig. 2.

The electrodes were made of a mylar film stretched tautly over a brass embroidery loop. A circular area, 11.3 cm^2, of each absorber was sprayed with a thin coat of graphite to give an electrically conducting lower surface.

On the top surface of the absorber a strip of graphite was painted leading from the metal hoop to two pinholes at the edge of the lower graphited area. This established electrical conductivity between the brass hoop and the graphited area on the lower side of the absorber. A fine wire in contact with the metal hoop was connected to the input of the vibrating reed

electrometer.

The coordinates of the center of the collecting electrode were established using a pointer mounted on a modified microscope stage. This device enabled the experimenter to center the particle with respect to the collecting electrode and ensured reproducible geometry.

The extrapolation chamber measurements were validated by comparison between the dose-rates obtained at NRDL and those obtained at Oak Ridge National Laboratory using an independently constructed extrapolation chamber. Good agreement between the data was assumed to indicate that the apparatus was free of important systematic errors. Before each series of measurements the apparatus was checked for consistency using a standard beta source.

The Beta-Dose Criteria and Models

The extrapolation chamber measurements yield average dose rates to a tissue-equivalent disk of an area equal to the area of the collecting electrode placed under the particle at a depth equal to the sum of the thicknesses of the top electrode and the absorber used (several absorbers ranging from 30 to 100mg/cm^2 were used during the course of this experiment). However, comparison with the existing dose criteria requires determination of the corresponding "point-depth dose" below the particle at a critical depth. This dose is defined as the energy imparted to an infinitesimally small volume surrounding the point directly underneath the particle at the critical depth. Using the density of the absorbing medium the point-depth dose is expressed in ergs per gram or in rads (1 rad is 100 ergs per gram).

The integrity of normal skin physiology is based in part on the mitotically active basal cell layer of epidermis. Acute lesions can result from disturbances of the kinetics of this population of cells. This basal, or "germinative," layer lies at the irregular interface of epidermis and dermis (see Figs. 5, 10); thus, the depth of the layer in human skin varies from point to point, ranging from about 20 to 250 microns. For convenience, a depth of 100μ was chosen to represent the critical level (12). The point-depth dose at 100μ has been used, therefore, as a yardstick for evaluating potential radiation damage to skin.

A survey by Krebs (12) has cited evidence that for an acute lesion of the skin to develop, the viable germinal cells must be reduced to a survival level of less than 0.001 over an area sufficiently large to prevent replacement of dead cells via cell proliferation in the margin of the exposure field. The provisional standard recommended by the Krebs study is that a dose to the skin of 1500 rads or more along the periphery of a circular field of 4 mm radius, 100μ deep in tissue, constitutes a potentionally hazardous exposure threat. Figure 7 is a diagram of this concept. As can be seen in the figure, the distance from the point of interception of the skin, by a line drawn from the center of the particle, to a point on the

circumference of a 4 mm radius circle, 100μ below the skin surface, is termed "Krebs' depth." This "depth" is obviously a derivative of the definition of a designated "point of interest." It has computational value in that it provides a correction for the presumed influence of particle geometry on dose. Clearly this "depth" has no intrinsic anatomic or physiologic significance and whether it provides a *necessary* correction remains to be seen.

Anatomically and physiologically, swine skin resembles human skin (3) and dose units apparently have equivalent significance in these two species. In contrast, the epidermis of the mouse is very thin and the integument has a dense covering of fine hair. Thus, while mouse skin is a sensitive indicator of radiation damage, it has no functional relationship to the Krebs concept. For convenience, our analyses of both pig and mouse data are based on point depth and Krebs' dose computations; other bases of analysis are being evaluated.

As mentioned previously, one of the main objectives of this study is to test both the substance and the quantitative aspects of these criteria. With the availability of experimental dose measurements and corresponding biological effects from this study, such an examination can be conducted if it is possible to transform the measured doses to their corresponding point-depth dose and Krebs dose. The Transmission-Degradation-Dissipation (TDD) beta dose model developed at NRDL (13) fulfilled the required transform function. The model is a combination of six separate and semi-independent computer codes. The first (Code 1) is a nuclide abundance program which solves a group of differential equations describing the buildup and decay of fission products developed from the uranium nuclei during reactor irradiation. Using input decay data, it also calculates the activity of each nuclide at the end of the irradiation period or at any time thereafter.

Code 2 computes the beta spectrum for each beta emitting nuclide when given the end-point energies, beta branching fractions, and degree of forbiddenness of the beta transitions. Output from the program is a sequence of value representing the probability that a beta particle will be emitted with an energy between E and E + ΔE, where ΔE = 0.01 Mev, and where values for E run from 0 to E Max. In practice these spectra have been generated and stored on tape for the composite spectrum program, Code 3 (below). The program is updated whenever new data appear in the literature.

Code 3 is a Composite Spectrum Program which sums the individual spectra of the 173 ^{235}U-fission product nuclides with appropriate weighting for the activity of each contributing nuclide as determined by the nuclide abundance program (Code 1). It produces a point-source spectrum at a given time and for given reactor conditions. Output from this program is a sequence of values representing the number of betas emitted by the source at each energy level.

The electron spectrum from a small spherical particle differs from that given by a point-source because the emergent beta particles are degraded in energy due to scattering and absorption processes within the particle.

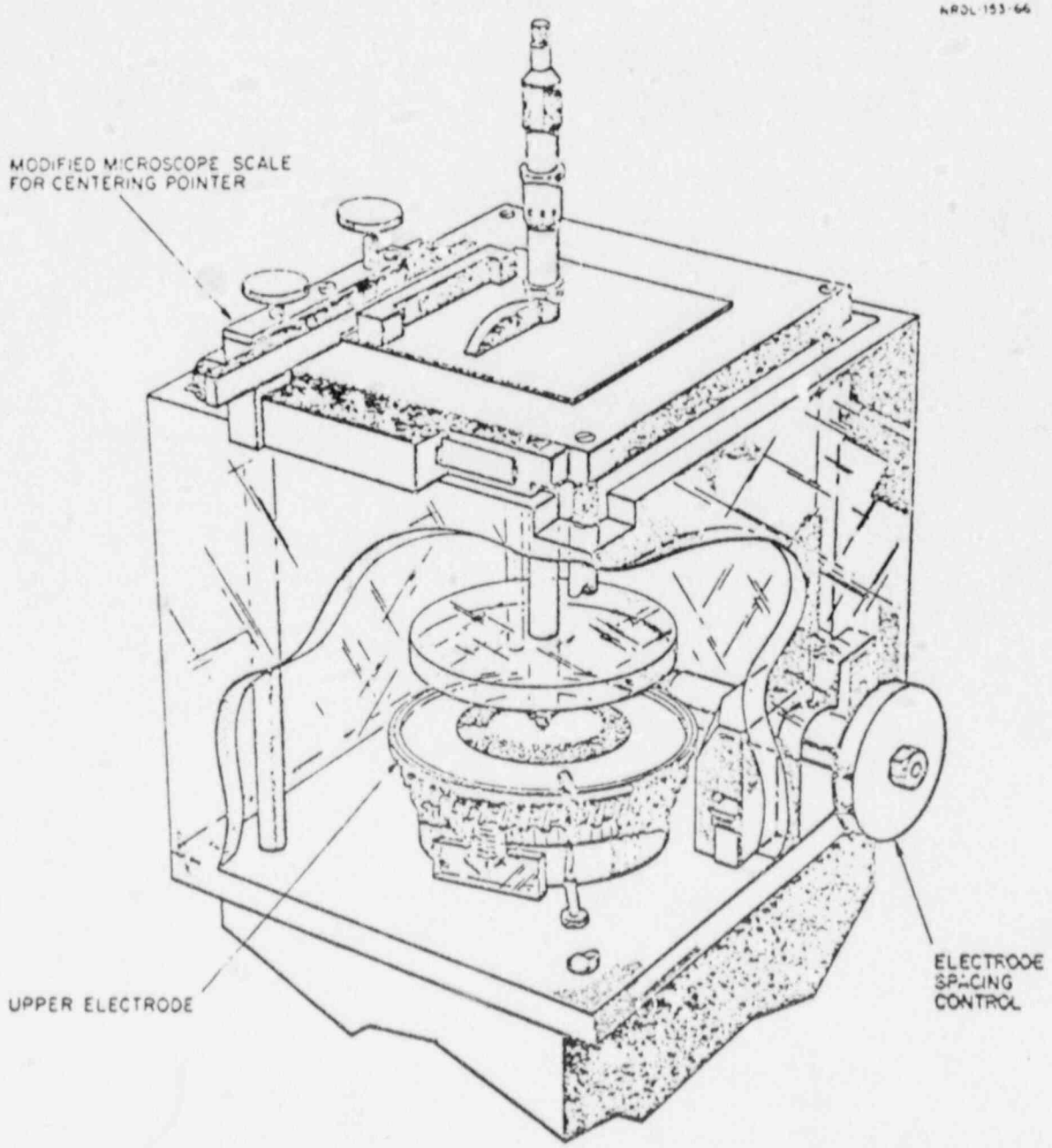

Figure 1. Schematic Diagram of the Extrapolation Chamber. (From Reference 12)

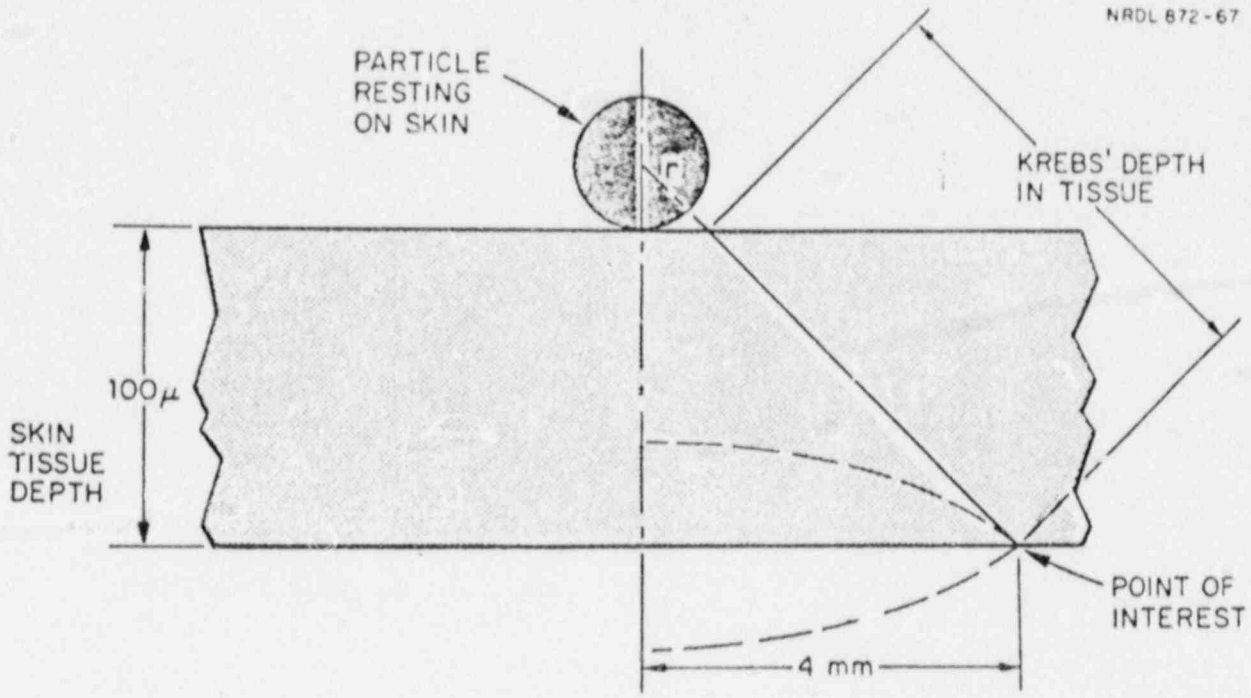

$$\text{'S' DEPTH} = \frac{100}{100+r}\sqrt{(100+r)^2+(4000)^2}\,\mu$$

Figure 2: Diagram of Krebs' Concept (not to scale).
From Reference 12
See also Figure 10.

This problem is handled by Code 4, a Monte Carlo code, which computes the loss in electron energy and number due to the absorption and scattering processes within the particle. These Monte-Carlo-determined losses are then applied to the composite beta spectrum from the point source of fission products by Code 5. The output is a beta spectrum emerging from a homogeneous, spherical particle of a specified size.

Code 6 uses the composite degraded spectrum emerging from the particle to compute the depth-dose-rate in tissue using the energy-dissipation factors for fast electrons as calculated by L. V. Spencer (14).

The equation for the dose-rate, D_t (in rads per hour), from a particle of volume V cm^3, emitting $N_e(E_o)$ betas/sec-cm^3 in the energy interval with mean energy E_o is:

$$D_t = \frac{kfgV_2}{4\pi Y} \sum_{E_o = \Delta E/2}^{E_o = E_{Max} - \Delta E/2} J(x)\,(dE/dr)_{E_o}\; N_e(E_o) \qquad (1)$$

Where:

k - is constant relating energy transport rate to dose-rate.
f - is a correction factor for a semi-infinite absorber, determined from an auxiliary Monte-Carlo program.
g - is the ratio of dose-rate at a distance Y from the center of a spherical source to the dose-rate from a point-source at the same distance from the detector.
J(x) - is Spencer's energy-dissipation-distribution function.
$(dE/dr)_{E_o}$ is the stopping power of the absorber (tissue, for example) for electrons emitted from the particle with energy E_o.

The final step of the model is to integrate the various dose-rates (from each energy range) with time to get doses. This is done by using time-integrated beta activities computed by the inventory code in making up the composite beta spectrum which is then degraded and deposited in tissue as explained above.

Doses computed by the model have been verified in several ways. A special report on this subject has been published (9).

As mentioned above, the beta dose-rate from each particle used in an animal exposure was measured on the extrapolation chamber soon

after its arrival at NRDL. In every measurement a series of readings of the ion current was taken as the size of the air gap was decreased. The ionization per cm^3 of air was determined from the limiting slope of the curve relating ionization current to the nominal air gap dimension (11). Almost all these curves were straight lines, a fact which increased our confidence in the validity of the measurements.

With the knowledge of the number of fissions per particle (as determined by the 4-pi ionization chamber), the particle diameter, its reactor activation time and duration, and its residence time on the animal, the TDD program was run to compute the dose-rate to a disk one inch in diameter, at a depth of 100μ in tissue (for direct comparison to the extrapolation chamber measurements), the point-depth dose 100μ in tissue underneath the particle, and the dose at Krebs' "point of interest" (Fig. 2). Compared with the beta dose rate, the gamma flux was considered low (11) and it was excluded from the computation. However, if the correction for "Krebs' depth" is assumed to be valid, then it would be expected that the gamma/beta ratio at the "point of interest" would rise steeply with decreasing particle size. Whether the gamma component has any biological significance has not been determined.

The point-depth doses and the corresponding Krebs doses for two experiments are listed in Tables II and III. For simplicity, only the Krebs dose will be mentioned in the text.

RESULTS AND DISCUSSION

Observations on Swine

Erythema

The site of each exposure was erythematous by the time the particles were removed from the skin. No effort was made to quantify the intensity of the change, but the extent of visible reddening was most intense and extensive by 24 hours, and it diminished during the next few days. Thereafter, erythema reappeared irregularly.

Epilation

Hairs continued to grow in the previously shaved skin surrounding treated areas, but all hair growth ceased in the skin displaying early erythema. By 30 days after exposure, some growth was evident again in the affected areas, and only the radiation scars were permanently epilated.

Pigment Changes

Darkening of normally pigmented skin formed a halo around the center of the exposed spot, beginning on the third day. The most intense darkening occurred before the end of the third week (Fig. 3),

and fading began thereafter. A narrow, irregular ring of hyperpigmentation remained permanently around the edge of the scar. The skin nearest the particle became involved in desquamation, followed by protracted healing. This area was permanently depigmented (Fig. 3).

Ulcer Formation

The disappearance of early erythema coincided with the appearance of one or more very small vesicles at the exposure site. These gave way to the formation of a single bulla which was always transient, usually granular in appearance, and somewhat variable in contour. With the loss of this surface material, each lesion then developed into an oozing sore indicating loss of functional epidermis. Cavitation of larger lesions provided evidence of loss of some dermis as well. The depth of damage would be expected to bear a direct relationship with the diameter of the lesion, and the appearance of the ulcers indicated that this was the case. A direct measurement of depth of lesions was not feasible, and quantitative data were based exclusively on surface dimensions.

None of the lesions was biopsied during the formation of the ulcer. Because cell and tissue events can only be inferred from clinical appearance, the extent of histologic destruction, as well as the precise mode of repair could not be determined. Consequently, the choice of a term to designate the lesions is an arbitrary one. The simplifying assumption was made that large and small lesions were qualitatively similar. Therefore, the word "ulcer" was chosen to designate one endpoint (see DISCUSSION for a fuller consideration of this problem). As used here, "ulcer" diameter is equivalent to the diameter of the denuded, oozing sore, and in turn, the diameter of the eschar which subsequently filled the denuded space.

The development of the lesion was more rapid at the sites of higher absorbed doses; in contrast, healing events appeared more rapidly after lower doses. Moist desquamation appeared at the sites of particle contact as early as the second day after exposure. The area of involvement gradually spread outward to its maximum size; the time required for full development was approximately two weeks for the smaller particles, and up to four weeks for the larger particles. Dry eschar formation commenced within three days after the appearance of an ulcer; by six weeks after exposure, all lesions were dry. Scarification was completed in most cases by twelve weeks. Residual evidence of damage included scars, flaking (radiodermatitis), depilation, and, in appropriate areas, pigment alterations. Reappearance of inflammatory changes was noted at irregular intervals, although healing proceeded with less complexity than that reported in much larger lesions (15).

TABLE II
Dosimetry Data and Responses (Lip Skin)

Particle Number	Particle Diameter (μ)	Exposure (hr:min)	Point Depth Dose 100μ in tissue (Rads)	Krebs' Dose (Rads)	Ulcer Diameter (mm)	Depigmentation Diameter (mm)
1	304	1:00	2.32×10^6	1.11×10^4	5	10
2	(fractured)	-	-	-	-	-
3	282	1:52	3.55×10^6	1.51×10^4	6	14
4	295	1:00	2.35×10^6	1.09×10^4	5	12
5	298	3:00	7.40×10^6	3.52×10^4	8	17
6	328	1:40	3.85×10^6	1.98×10^4	7	20
7	294	2:03	3.80×10^6	1.73×10^4	6	14
8	305	0:41	1.53×10^6	7.32×10^3	5	12
9	283	0:30	$1.2[illegible] \times 10^6$	5.40×10^3	4	8
10	308	0:30	1.51×10^6	7.49×10^3	5	10
11	149	3:05	1.70×10^6	2.88×10^6	4	8
12	150	3:00	1.37×10^6	2.31×10^3	3	9
13	148	0:30	2.40×10^5	4.05×10^2	0.5	1
14	140	0:30	2.86×10^5	4.44×10^2	0.5	2.5
15	152	1:30	6.42×10^5	1.06×10^3	2	5
16	148	1:00	5.69×10^5	9.44×10^2	0.5	3
17	153	1:28	5.14×10^5	7.71×10^2	2	5
18	145	1:00	4.88×10^5	7.70×10^2	1	5
19	154	1:45	7.17×10^5	1.21×10^3	2	6
20	144	1:28	5.63×10^5	9.21×10^2	0.5	5

TABLE III
DOSIMETRY DATA AND RESPONSES (MOUSE)

Mouse Number	Particle Number	Particle Diameter (u)	Exposure (Minutes)	Point Depth Dose 100u in tissue (Rads)	Krebs' Dose (Rads)	Hair Growth Delay Diameter (mm)
1	11	141	25	1.04×10^5	1.55×10^2	5
2	3	286	17	2.82×10^5	1.19×10^3	(biopsied)
3	1	293	18	2.82×10^5	1.23×10^3	7
4	12	146	24	1.20×10^5	1.88×10^2	5.5
5	5	304	25	5.46×10^5	2.49×10^3	7
6	1	293	12	1.67×10^5	7.23×10^2	8
7	12	146	14	6.00×10^4	9.27×10^1	3.5
8	5	304	14	2.60×10^5	1.18×10^3	9
9	11	141	13	4.66×10^4	6.78×10^1	4.5
10	2	287	07	1.08×10^5	4.53×10^2	5
11	13	148	13	5.79×10^4	9.12×10^1	3.5
12	4	288	13	1.53×10^5	6.50×10^2	5
13	3	286	13	1.91×10^5	8.03×10^2	(biopsied)
14	12	146	28	1.05×10^5	1.59×10^2	3.5
15	5	304	28	4.51×10^5	2.02×10^3	9
16	1	293	29	3.51×10^5	1.51×10^3	(biopsied)
17	11	141	29	9.60×10^4	1.30×10^2	5
18	13	148	27	1.05×10^5	1.64×10^2	4.5
19	4	288	15	5.35×10^4	8.69×10^1	7
20	3	286	28	3.60×10^5	1.49×10^3	(biopsied)
21	7	277	08	1.01×10^5	4.37×10^2	5
22	17	154	08	3.66×10^4	6.17×10^1	3.5
23	2	287	25	3.44×10^5	1.44×10^3	7
24	20	142	04	1.31×10^4	1.31×10^4	3.5
25						(died)
26	2	287	05	6.12×10^4	2.54×10^2	5.5
27	18	141	14	4.75×10^4	6.86×10^1	3.5
28	8	293	15	2.24×10^5	9.68×10^2	5
29	19	151	15	5.35×10^4	8.69×10^1	3.5
30	17	154	17	7.19×10^4	1.20×10^2	2
31	7	277	16	2.03×10^5	8.01×10^2	7
32	20	142	20	6.08×10^4	8.83×10^1	(biopsied)
33	6	318	20	2.78×10^5	1.31×10^3	7
34	14	150	23	6.52×10^5	1.03×10^2	4.5
35	15	138	12	2.49×10^4	3.43×10^1	1.5
36	15	138	17	5.66×10^4	7.51×10^1	1.5
37	10	304	22	3.07×10^5	1.38×10^3	9
38	18	141	22	$6.[illegible] \times 10^4$	9.50×10^1	3
39	6	318	24	1.75×10	8.20×10^2	(biopsied)
40	20	142	14	3.85×10^4	5.51×10^1	2
41	19	151	12	3.70×10^4	5.87×10^1	5.5
42						(died)
43	7	277	13	1.51×10^5	5.92×10^2	5
44	17	154	12	4.66×10^4	7.68×10^1	2
45	15	138	12	2.32×10^4	3.17×10^1	2
46	8	293	12	1.54×10^5	6.60×10^2	4

Figure 3. Hot particle-induced lesions in pig skin. Frames numbered left to right & top to bottom.

Frame 1. Photographic technique for recording changes in lesions. Fixed-distance close-up camera assures identical format for each frame.

Frame 2 through 7. Particle exposure #19 (Krebs' dose 1.20×10^3 rads). Photographs taken on the following days post-exposure: 13, 21, 24, 26, 45, 66. Magnification: 1.4x.

Frames 8 through 15. Particle exposure #11 (Krebs' dose 2.88×10^3 rads). Days post exposure: 0, 13, 17, 21, 26, 29, 41, 66.

Frames 16 through 25. Particle exposure #5 (Krebs' dose 3.51×10^4 rads). Days post-exposure: 0, 7, 9, 13, 19, 21, 26, 29, 36, 61.

Frame 26. Particle exposure #13 (Krebs' dose 4.05×10^2 rads). Photograph was taken on day 49.

Frame 27. Particle exposure #3 (Krebs' dose 1.50×10^4 rads). Photograph was taken on day 49 (see also Fig. 8 and histologic description in text).

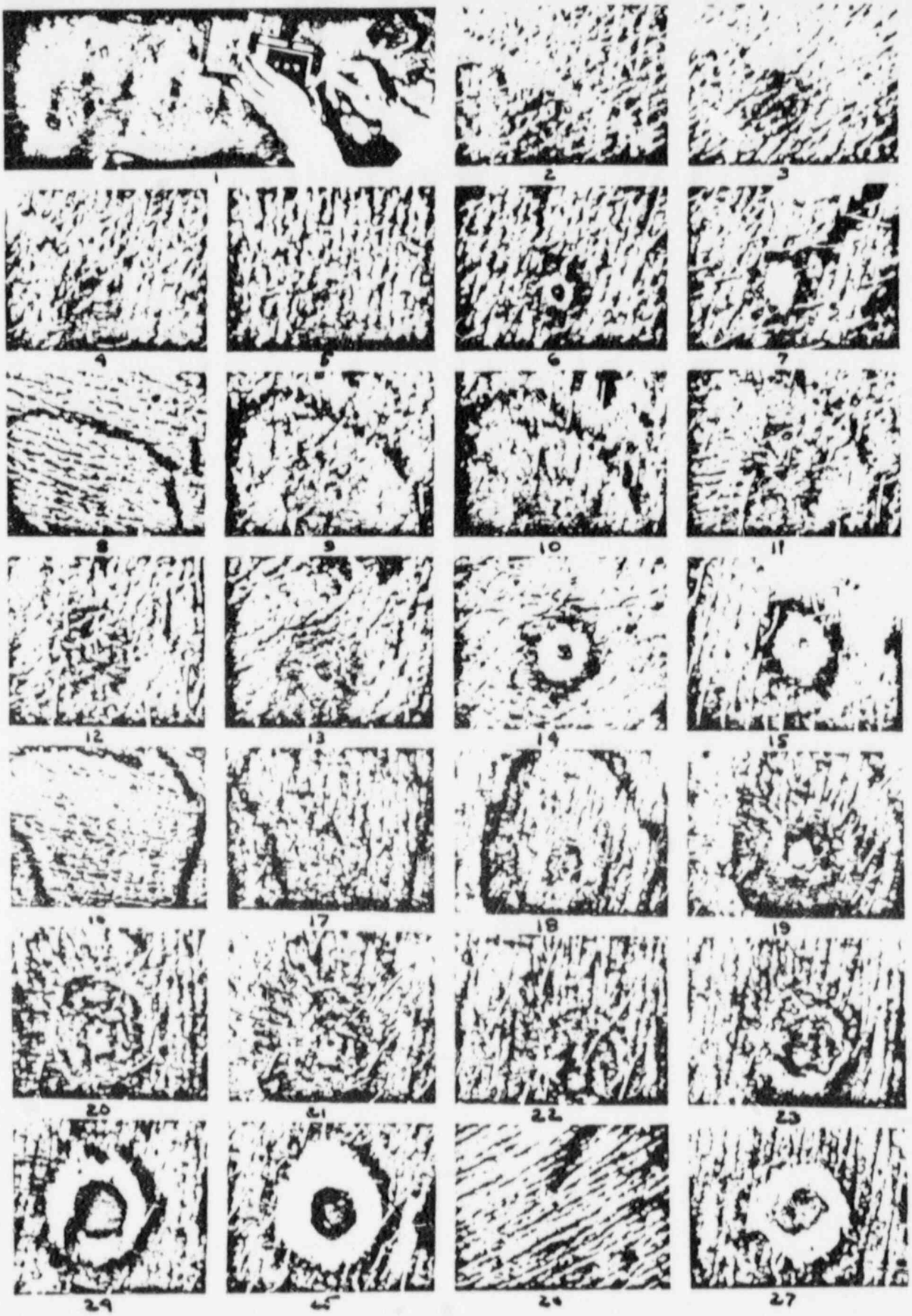

Fig. 3

Quantitative Response

Dose-response curves for diameters of ulcer formation (UF) and depigmentation (DP) are shown in Fig. 4. These endpoints are strongly correlated with dose, and, not surprisingly, with each other (for UF vs. DP, r = 0.95).

Histopathology

Two excision biopsy specimens were removed from pigs during the course of the final experiments. The first (Spot #3) had received 15 x 10^3 rads (Krebs') 55 days previously. A photograph of the skin surface is contained in Fig. 3, and the histologic appearance is shown in Fig. 8. Histologically, the lesion had sharply defined borders on the lateral edges, but it merged gradually into the connective tissue below. Tongues of epithelium from the surrounding epidermis could be seen growing in under the eschar. The regenerating epithelium was vascularized and hypertrophic with a rather thick stratum corneum. The epidermis immediately adjacent to the eschar and its overlying stratum corneum was amelanotic, although a few scattered DOPA-positive cells were present. Hypertrophy and bizarre mitotic figures were present. Abnormal amounts of melanin were contained in cells surrounding the vascular elements of the superficial dermis. Further from the eschar, there was an abrupt transition from hypopigmented to hyperpigmented epidermis. The peripheral area contained excessive amounts of melanin in both epidermis and stratum corneum; some pigmented cells were present in the dermis. The epidermis of the hyperpigmented area was only slightly hypertrophic.

Site #13 was also biopsied at 55 days post-treatment. The Krebs dose was 405 rads, and the ulcer had not exceeded 0.5 mm diameter. As was characteristic with the smaller lesions, healing was well underway. However, the lesion was qualitatively similar to the one described above, confirming the clinical impression that the radiation burns presented a continuum down to the smallest ulcers produced.

III.2 Observations on Mice

Qualitatively, most of the changes occurring in exposed mouse skin were similar to those seen in pig skin. However, comparable changes were elicited by much lower doses in mice, probably as a function of their thinner epidermis (Fig. 9). Inhibition of hair growth in mice is produced by relatively small doses of radiation (Fig. 5). The location and extent of damage was readily identified in the black-haired mice (Fig. 6, 7). Rhino mice have a life expectancy of approximately 10-12 months (4). Eleven months after the exposure of a group of 10 rhino mice, the lone survivor developed a tumor at the site of particle contact. The estimated Krebs dose was 190 rads, and in the acute phase, an ulcer of less than 0.5 mm had developed.

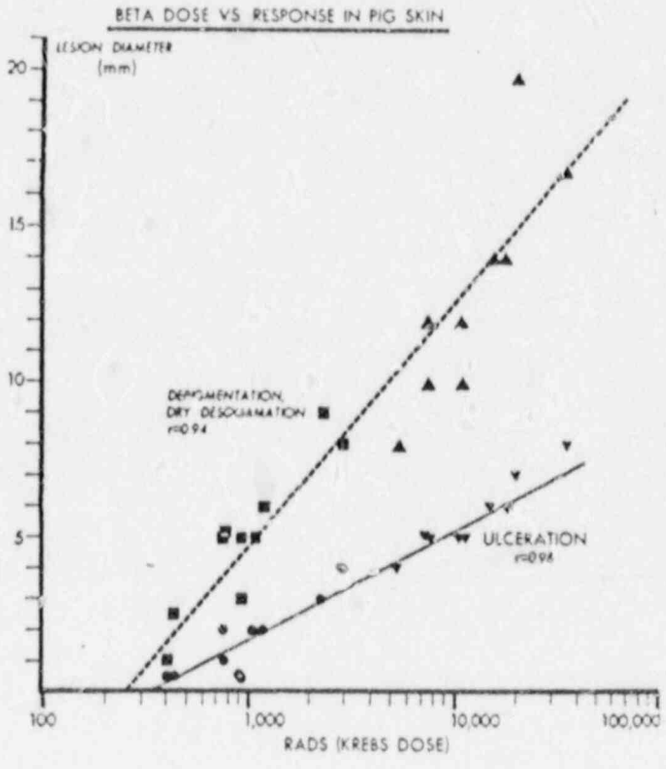

Figure 4. Small particles are represented by squares and circles. Large particles are represented by triangles. Curves fitted by least squares analysis (Ref. 16).

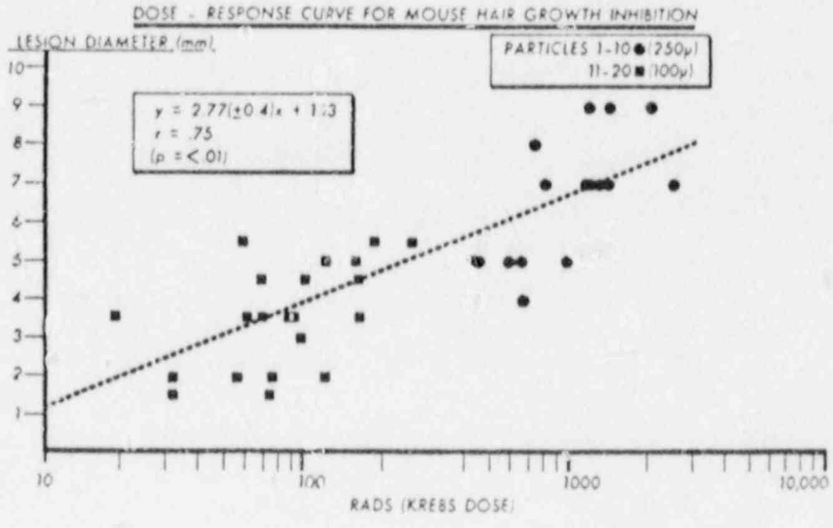

Figure 5. Large particles represented by circles, small particles represented by squares.

Discussion

In evaluating specific radiation hazards, it has sometimes been difficult to extrapolate from available data. For example, the degree of damage which could be expected from cosmic ray heavy nuclei posed a problem apparently not answerable from data on large-field radiation exposures. Consequently, Chase and Straile (17) and later Curtis et al. (18) developed methods for exposing skin and other tissues to collimated microbeams of x-rays. In terms of equivalent absorbed doses, the response of tissue in such limited areas proved to be qualitatively different from that of tissue under conventional techniques.

The evaluation of radioactive microspheres ("hot particles") as a potential source of external radiation poses an analogous problem. Existing data on large field studies, sieve and grid exposures, and microbeams are probably insufficient for estimating acute responses and are almost certainly inadequate for the predicting of such late effects as carcinogenesis from hot particles. Relative to the size of the system being exposed, the hot particle may be represented reasonably well as a point source. Even if the emission from such a source were monochromatic, the absorbed doses at various distances would present a rather complex array of isodose curves influenced by distance and various absorber densities. The dosimetry problem is further complicated if the particle contains a mixture of isotopes.

Absorbed radiation is presented here as the "point-depth dose" 100μ below the particle and as the "Krebs dose." The distances involved are illustrated in Fig. 10 in proportion to one particle 300μ in diameter and another particle 86μ in diameter. The "sensitive" layer of skin is represented schematically by the bar of tissue 100μ thick since germinative cells and blood vessels supplying the epidermis of human and pig skin are, on the average, at that depth. Tissue absorption and distance account for the very significant difference between the point-depth and Krebs' doses from the same particle. The ratio of one dose to the other is a function of the particle size as well as the composite spectrum which is, in turn, dependent on the exposure time and duration. Although the Krebs dose provides a better visual image of dose fall-off with distance, the two methods correlated about equally well with the biologic responses recorded during this project (Table IV). However, under the conditions of these experiments, the two methods could not be exhaustively compared. Krebs' criterion, which carries with it the idea of area damage vs. a dose to a small volume around a point, has the apparent advantage of correcting for the effect of particle size (and thus the comparative path lengths in air and tissue) on absorbed dose (Fig. 10). For this reason, a fairer test of the Krebs model would involve an experiment in which the full range of doses would be delivered by both large and small particles. At present, we have available for analysis only high doses delivered by large particles, and lower doses by small particles.

TABLE IV

CORRELATION COEFFICIENTS (r)

	Mouse Hair Growth Inhibition	Pig Skin	
		Ulcer	Depigmentation, Desquamation
Krebs' Dose	0.75	0.98	0.94
Point Depth Dose	0.74	0.96	0.94

Ionizing radiations, including beta particles, have induced cancer in skin (19-22). Although there had not yet emerged a clear basis for evaluating the skin cancer risk of a specified hot particle incident, Krebs' provisional description of a potentially hazardous exposure was employes (11); the production of a radiation-ulcer was emphasized mainly because it was felt that "cancer of the skin is consistently associated with the development of serious, non-healing or recurring, acute lesions of the skin." (12)In turn, the preoccupation of this report with Krebs' doses and radiation ulcers is a result of an attempt to produce data on ulcer dose "thresholds" comparable to those cited above (12).

A variety of designations have been used in referring to skin lesions produced by radiation. Krebs (12)chose to use the categories employed primarily by British workers: I (*Erythema*), II (*Dry Desquamation*), III (*Moist Desquamation*), IV (*Ulceration*). Other sources qualify category IV as *severe* ulceration, and add a fifth category (V *Necrosis*). Category V is considered to involve infection and other impediments to healing (23).

The bleeding lesion shown in Frame 20 of Fig. 3 would fit Category IV (*Ulceration*, as described in References 12 and 23). The lesion shown in Frame 26 had passed through a stage characterized by moist desquamation (Category III). Qualitatively, it was similar to the larger lesions, but on the basis of its size, it is doubtful whether such a lesion would generally be called a severe ulcer. It is probable that for particle-induced lesions, Category IV ceases to exist somewhere between these extremes in size, and this possibility should be explored experimentally.

A model describing the radiation response for epidermal cell populations in mouse skin influenced the predictions of dose-response following particle exposure (12). Further evidence for the validity of the mouse model has been presented by Emery et al. (24), although Archambeau and Mathieu (17) have given evidence from work in swine that available radiation-response models for skin are not entirely satisfactory. Coupled with the complexities in dosimetry models for point sources, these facts appear to underline the uncertainties that necessarily exist in interpreting and predicting particle-induced skin lesions.

Figure 6. $C_{57}BL$ mouse plucked (during telogen phase of hair cylce) and exposed 9 days before picture was taken. Krebs' dose 1.44×10^3 rads. Central eschar is surrounded by area of retarded hair growth.

Figure 7. Twelve days post-exposure, Krebs' dose 1.17×10^3 rads. Darker surrounding area indicates further hair growth in unaffected skin.

Figure 8. Photomicrograph of pig skin at site of exposure #3. Eschar appears on right, edge of ulcer at center, and peripheral skin is at left of photograph. See more detailed description in text. (H&E stain; scale shows one millimeter).

Figure 9. Rhino mouse, 7 days following a Krebs' dose of 1.78×10^3 rads.

7

6

9

8

Because all the skin exposures from these experiments resulted in ulcers as defined previously and with further experiments on uranium particles precluded by the closing of NRDL, the existence of a threshold dose remains hypothetical. The data derived up to that time could be interpreted to indicate that 1) the minimum dose required to produce a small but recognizable ulcer is below 405 rads (Krebs) and 2) assuming a continued straight-line relationship, the UF and the DP approach zero at about 350 rads and 250 rads respectively (Fig. 4). However, it has not been determined from available data whether deviations exist at the origin end of the curve and so the extrapolation must be interpreted with caution.

Testing the dosimetry models (12, 25) for acute damage is an operational matter, totaly dependent on available materials. However, as Krebs has pointed out, there are no experimental data available which clarify the possible relationship between either absorbed dose or surface area response and the effects following exposure to hot particles; e.g., cancer. Therefore, any judgment now on the ultimate significance of these skin lesions would be premature.

Figure 10. Diagram showing relationships implied by the Krebs' concept.

A. Krebs' concept drawn to scale. The average epidermal thickness is represented by the dashed lines. Solid lines are drawn from the centers of two particles to a point 4 mm lateral and 100 microns deep. That portion of the solid line within the "epidermis" is termed the Krebs' depth, and it is significantly influenced by particle size.

B. Schematic representation of swine epidermis, drawn to the same scale as above. Epidermal ridges and cones, enclosing the vascularized dermal papillae, produce the irregular wavy line which characterizes the undersurface of the epidermis. In addition, naturally-occurring creases in the skin distort the entire epidermis into a series of hills and valleys.

C. Krebs' concept superimposed on diagram of swine epidermis. The local configuration of the skin, as well as the location of the particle, can influence absorbed dose at any significant distance.

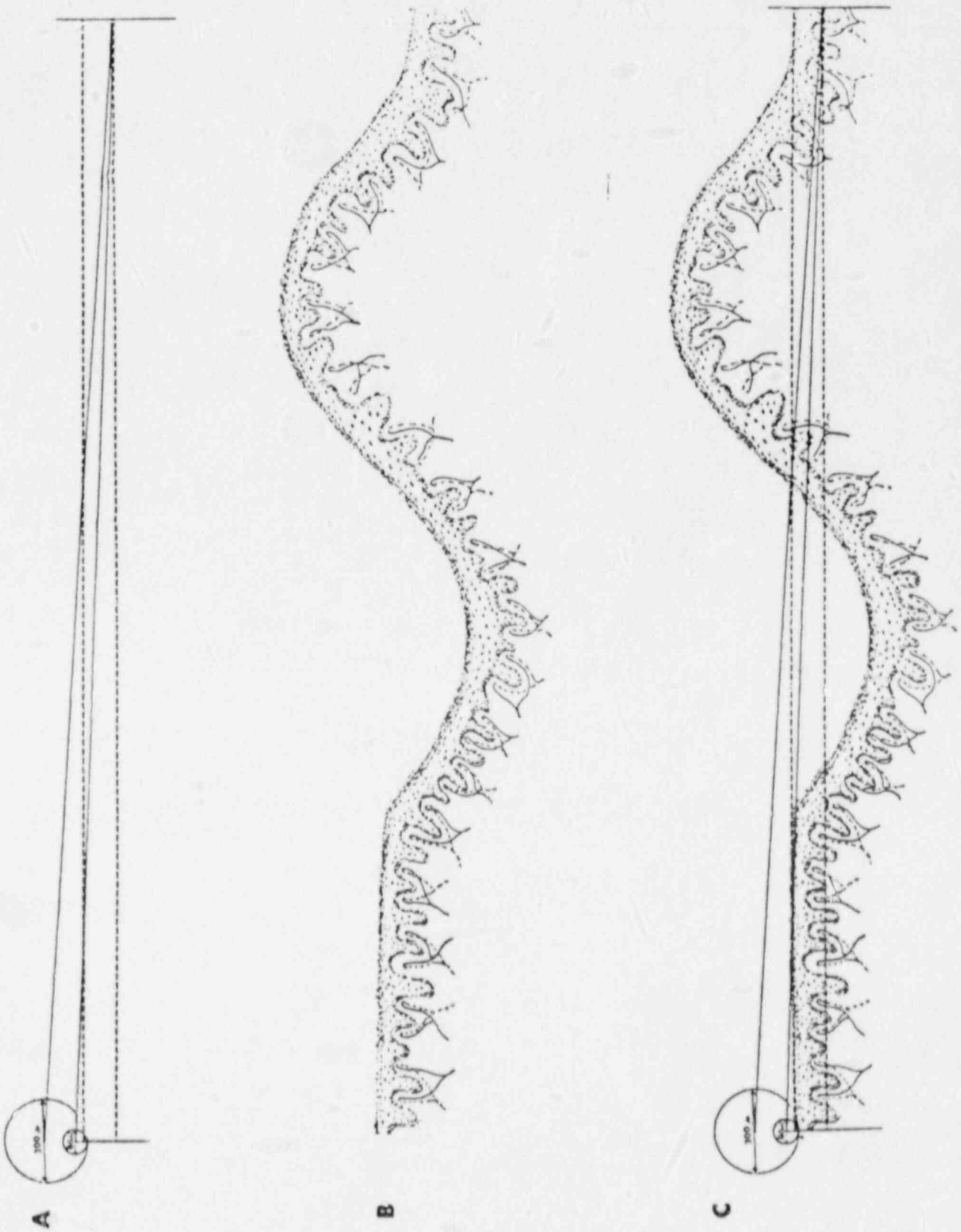

29

Fig. 10

References

1. Charles, M. W. 1976. A Study of Carcinogenic Risks Following The Non Uniform Irradiation of Skin. I: An Appraisal of Theoretical Models (Report RD/B/N3484 Central Electricity Generating Board Research Dept. Berkeley Nuclear Laboratories). II: A Proposal For an Animal Experiment (Report RD /B/N3633 Central Electricity Generating Board Research Dept. Berkeley Nuclear Laboratories).

2. Forbes, P. D. 1977. II. ^{90}Strontium Silicate Microspheres. In preparation.

3. Forbes, P. D. 1967. Radiation Effects in Swine. I. Vascular Supply of the Skin and Hair. U.S. Naval Radiological Defense Laboratory, USNRDL-TR-67-141.

4. Forbes, P. D. 1965. Experimentally-Induced Neoplasma in the Skin of Mice. I. Single-Dose Effects of DMBA in Haired, Hairless, and Rhino Mice. J. Invest. Dermatol. 44:388-398.

5. Johnson, W. D., P. D. Forbes, J. H. Graham, and H. R. Gray. 1966. Experimental Cutaneous Calcinosis: A Histopathologic and Histochemical Study. J. Invest. Dermatol. 43:453-466.

6. Jones, J. W. and R. T. Overman. 1948. Use and Calibration of 100% Geometry Ion Chamber. Oak Ridge National Laboratory, AECD-2367.

7. Miller, C. F. 1957. Response Curves for USNRDL 4-pi Ionization Chamber. U. S. Naval Radiological Laboratory, USNRDL-TR-155.

8. Mackin, J. L., L. W. Weisbecker, and P. E. Zigman. 1965. Radionuclide Release from Aero-Space Nuclear Reactor Fuels II. Phase One: Pulsed Neutron Irradiation of Dry Fuel. U. S. Naval Radiological Defense Laboratory, USNRDL-TR-911, 18 January.

9. Mikhail, S. Z. 1970. Tissue Beta Radiation Doses From Particulate Fission Product Sources: Comparison of Model Predictions With Experimental and Monte Carlo Values. ESA-TR-70-01 Environmental Science Associates Technical Report.

10. Loevinger, R. 1953. Extrapolation Chamber for the Measurement of Beta Sources. Rev. Sci. Instr. 24:907.

11. Mikhail, S. Z. and K. A. Collins. 1968. Analysis of the Particulate Effluent Data From Phoebus IB,EP-IV Nuclear Reactor Test. U. S. Naval Radiological Defense Laboratory, USNRDL-TR-68-23.

12. Krebs, J. 1967. The Response of Mammalian Skin to Irradiation with Particles of Reactor Debris. U. S. Naval Radiological Defense Laboratory, USNRDL-TR-67-118.

13. Ulberg, J. D. and D. B. Kochendorfer, 1966. Models for Estimating Beta Dose to Tissue from Particle Debris in Aerospace Nuclear Applications. U. S. Naval Radiological Defense Laboratory, USNRDL-TR-1107.

14. Spencer, L. V. 1959. Energy Dissipation by Fast Electrons. National Bureau of Standards, NBS Monograph 1, 1 September.

15. Archambeau, J. O. and G. R. Mathieu. 1969. Comparison of the Observed Results of Irradiation on the Skin With Those Expected from an Idealized Model. Rad. Res. 40:285-297.

16. Snedecor, George W. 1956. Statistical Methods. The Iowa State College Press.

17. Straile, William E. and Herman B. Chase. 1963. The Use of Elongate Micro Beams of X-rays for Simulating the Effects of Cosmic Rays on Tissue: A Study of Wound Healing and Hair Follicle Regeneration. Rad. Res. 18:65-75.

18. Curtis, Howard J. 1967. The Use of a Deuteron Microbeam for Simulating the Biological Effects of Heavy Cosmic-Ray Particles. Rad. Res. 32:250-257.

19. Traenkle, Herbert L. 1962. X-ray-Induced Skin Cancer In Man. NCI Monograph 10:423.

20. Hulse, E. V. 1967. Incidence and Pathogenesis of Skin Tumors in Mice Irradiated with Single External Doses of Low Energy Beta Particles. Br. J. of Cancer:21, No. 3.

21. Albert, R. E., M. E. Phillips, P. Bennett, F. Burns and R. Heimbach. March 1969. The Morphology and Growth Characteristics of Radiation-Induced Epithelial Skin Tumors in the Rat. Cancer Research 29:658-668.

22. Schubert, G., H. A. Kunkel and G. Uhlmann. 1955. Carcinogenic Action of Different Doses of Local β-Ray Irradiation, Progress in Radiobiology, edited by Joseph S. Mitchell, Barbara E. Holmes and Cyril L. Smith. Charles C. Thomas, Springfield. pp. 480-484.

23. Rubin, Philip and George W. Casarett. 1968. Skin and Adnexa, Chapt. 3 in Clinical and Radiation Pathology. W. B. Saunders Co., Philadelphia.

24. Emery, E. W., J. Denekamp, and M. M. Ball. 1970. Survival of Mouse Skin Epithelial Cells Following Single and Divided Doses of X-rays. Rad. Res. 41:450-466.

25. Sanders, Charles L., Roy C. Thompson and W. J. Bair. 1969. Carcinogenesis in the Lung From Inhalation of Radioactive Particles Report Contract N00228-68-1421 to USNRDL (CFSTI Document #AD690[illegible]).

VII APPENDIX

BACKGROUND OF THIS PROJECT

Contract SNPN-49 (Formerly N00 228 69 C 1303)

In his paper (USNRDL-TR-67-118, 1967) on possible hazards of hot particles, Krebs indicated the need for experimental studies on animals. A detailed work plan for this type of research program was required, and, under contract #N00 228 68 C 0571, the Radiology Department of Roger Williams General Hospital agreed to develop the research plan. It was anticipated that the proposed experimental design should be modified as the result of preliminary trials under laboratory conditions. For this purpose, the U. S. Naval Radiological Defense Laboratory supplied three batches of pyrocoated enriched uranium carbide beads, and the contractor agreed to make preliminary determinations of acute skin changes.

Several techniques for handling hot particles and for keeping them in contact with the skin of swine were tested. During 5 reactor experiments 44 particles were activated and some of the particles were used in the exposure of several types of photographic film, as well as the irradiation of skin on 20 mice and 5 swine. One batch of particles (designated "third shipment") was used in the last of the experiments conducted at the Rhode Island Nuclear Science Center. This final experiment involved the use of 12 particles and the evaluation of the 12 lesions produced by them. The particles were returned to NRDL for dosimetry determinations, and the biological and physical data were exchanged between the laboratories. Using least squares analysis, and assuming linearity over the entire range of particles used, a curve was adequately described by the equation $Y = 11.18 \text{ Log } X - 9.06$, where X was the Krebs dose in rads and Y was the ulcer diameter in millimeters ("ulcer" and "Kreb's dose" are described in detail in the body of this report). The studies were briefly summarized in the final project report, and also in a published abstract (Radiation Research 39:Abstr. De-8, 1969, reproduced on the following page). On the basis of these studies, a detailed work plan was drawn up and submitted in fulfillment of the contract terms. The project support period was 90 days, although the contract was extended to nine months (with no added cost to the government) to allow for a longer evaluation of the biologic changes. The research program was transferred when Dr. Forbes moved to Temple University.

The detailed work plan (entitled Acute Leions in Skin Produced By Radioactive Microspheres, Phase II) became the basis for the contract resulting in this report. Navy Contract #N00 228 69 C 1303 was designed to fund an abbreviated (six-month) study of particle effects. Three experiments were run before the abrupt cessation of research activities at NRDL terminated the supply of UC_2 particles. A higher degree of confidence in dosimetric techniques had been gained by the time these experiments were completed, and the results are presented in this report.

Reprinted from RADIATION RESEARCH, Volume 39, No. 2, August 1969

Dec. 8. *Effects of Single Radioactive Microspheres on Skin.* P. DONALD FORBES. The Skin and Cancer Hospital, Temple University Health Science Center, Philadelphia, Pennsylvania 19140.

Tissue effects were evaluated after activated uranium microspheres (80–301-μ diameter) were applied to the skin of swine. Radiation doses were calculated for several tissue depths, utilizing a mathematical model (S. Z. Mikhail and K. A. Collins; USNRDL-TR-68-23 1968). At a point 4 mm lateral to the particle and 100 μ deep in skin, doses ranged from 7×10^2 to 16×10^3 rads, as a function of particle size and exposure time. Ulcers, beginning at the site of contact, eventually became 2–12 mm in diameter. Pigmentation changes, hair follicle dysplasia, desquamation, scarification, and reulceration were some of the other dose-dependent responses.

The physical features of absorbed dose in skin are complicated by a heterogeneous and complex tissue anatomy, uncertain locations of presumptive targets, and physiologic responses such as cell alteration, death, and repopulation. Nevertheless, dosimetric models based on computer routines have led to increased confidence in the elaboration of "point source" isodose patterns. We are investigating the reconciliation of dosimetry models with observed biologic responses, and the practical feasibility of predicting acute and chronic skin changes resulting from exposure to very small radioactive sources. (Supported in part by USNRDL Contract N00 228-68(C)571.)

Reprinted from Radiation Research, Volume 39, No. 2, August 1969
Copyright © 1969 by Academic Press, Inc. *Printed in U.S.A.*

De 8. *Effects of Single Radioactive Microspheres on Skin.* P. Donald Forbes, The Skin and Cancer Hospital, Temple University Health Science Center, Philadelphia, Pennsylvania 19140.

Tissue effects were evaluated after activated uranium microspheres (86–301-μ diameter) were applied to the skin of swine. Radiation doses were calculated for several tissue depths, utilizing a mathematical model (S. Z. Mikhail and K. A. Collins; USNRDL-TR-68-23 1968). At a point 4 mm lateral to the particle and 100 μ deep in skin, doses ranged from 7×10^2 to 16×10^3 rads, as a function of particle size and exposure time. Ulcers, beginning at the site of contact, eventually became 2–12 mm in diameter. Pigmentation changes, hair follicle dysplasia, desquamation, scarification, and reulceration were some of the other dose-dependent responses.

The physical features of absorbed dose in skin are complicated by a heterogeneous and complex tissue anatomy, uncertain locations of presumptive targets, and physiologic responses such as cell alteration, death, and repopulation. Nevertheless, dosimetric models based on computer routines have led to increased confidence in the elaboration of "point source" isodose patterns. We are investigating the reconciliation of dosimetry models with observed biologic responses, and the practical feasibility of predicting acute and chronic skin changes resulting from exposure to very small radioactive sources. (Supported in part by USNRDL Contract N00 228-68-C057.)